Numerical scalings of the decay lengths in the Scrape-Off Layer

F. Militello[1], V. Naulin[2], A.H. Nielsen[2]

[1] *EURATOM/CCFE Fusion Association Culham Science Centre, Abingdon, UK*

[2] *Association EURATOM-DTU, Technical University of Denmark, Roskilde, Denmark*

One of the major concerns for the next generation tokamaks and for the future fusion reactors is the exhaust of heat and particles. This process controls the plasma flow from the core towards the first wall and the divertor, and determines the longevity of the plasma facing components as well as the overall performance of the machine. The physics of the exhaust is regulated by the narrow region of plasma known as the Scrape-Off Layer (SOL), where field lines do not close on themselves, but impinge on solid surfaces. Due to the presence of open field lines, the radial width of the SOL is determined by the balance between the parallel and the perpendicular transport. In L-mode, the latter is caused by turbulence, and in particular by coherent structures (called filaments or blobs) generated inside the last closed flux surface and expelled into the SOL. The SOL width is a meaningful quantity as it determines the wetted surface on the divertor target, over which the power exhausted from the core is deposited. In other words, it determines the typical decay length of particles and energy outside the separatrix.

We studied the perpendicular transport at the outer midplane using a simplified interchange model which allows to reproduce the blob dynamics in the SOL. In particular, we performed a systematic numerical campaign with the code ESEL [1] in order to determine the power decay length for different plasma regimes. We then applied regression analysis in order to extract scaling laws for the SOL width from our large database of L-mode turbulence simulations.

The model used is based on 2D drift-fluid equations describing the evolution of the plasma density, n, electron temperature, T, and vorticity, U:

$$\frac{\partial n}{\partial t}+\frac{1}{B}[\phi,n] = nC(\phi)-C(nT_e)+D\nabla_\perp^2 n-\Sigma_n n, \qquad (1)$$

$$\frac{\partial T}{\partial t}+\frac{1}{B}[\phi,T] = \frac{2}{3}TC(\phi)-\frac{7}{3}TC(T)-\frac{2}{3}\frac{T^2}{n}C(n)+\chi\nabla_\perp^2 T-\Sigma_T T, \qquad (2)$$

$$\frac{\partial \Omega}{\partial t}+\frac{1}{B}[\phi,\Omega] = -C(nT_e)+\mu\nabla_\perp^2\Omega-\Sigma_\Omega\Omega. \qquad (3)$$

Here, $\Omega=\nabla_\perp^2\phi$, where ϕ is the electrostatic potential, C is a curvature operator responsible for the interchange dynamics, the brackets are standard Poisson brackets used to describe the advection. In addition, the inverse of the magnetic field $B^{-1}\approx 1+\varepsilon+(\rho_s/R)x$, where ε is the inverse aspect ratio, ρ_s is the ion sound Larmor radius, R is the major radius and x is the "radial" coordinate. The equations are solved in a drift plane ideally located at the outer midplane. The parallel dynamics is not solved self-consistently, but it is represented by simplified loss terms on the left-hand side of Eqs.1-3. All the quantities are dimensionless as Bohm normalization was applied to the equations. More details about the model are discussed in [1, 2].

Note that once the boundary conditions (described in [2]) are fixed, the solution of Eqs.1-3 is uniquely determined by the seven dimensionless parameters that appear in the equations. These are the machine inverse aspect ratio, ε, the interchange drive (the curvature operator is proportional to it), ρ_s/R, the particle and thermal diffusivity, D and χ, the viscosity, μ, the particle and momentum parallel loss term, $\Sigma_n = \Sigma_\Omega$ and the temperature parallel loss term, Σ_T. These parameters were systematically varied in order to explore a parameter space that was relevant for small and medium machines (see Fig. 1). Note, however, that $\varepsilon = 0.67$ in all our simulations as we wanted to investigate spherical tokamaks. Our conclusions are nevertheless applicable to standard configurations as a slightly different ε would only change the constant factor in front of the scaling laws [3].

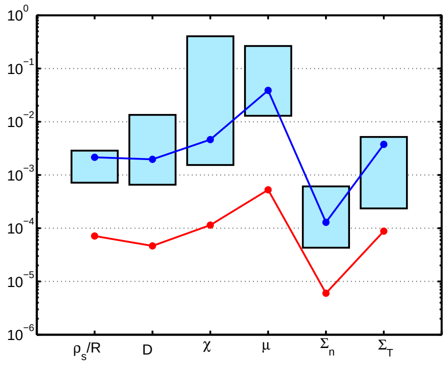

Figure 1: The boxes represent the variation range of the dimensionless parameters in our simulation database. The blue (red) curve is representative of MAST (ITER).

We briefly summarize the numerical set up of the simulations, which is discussed in detail in [3]. Equations 1-3 are solved in slab domain representing the drift plane. The "radial" coordinate spans $150\rho_s$, the first 50 of which represent the edge region inside the separatrix where interchange instabilities drive the turbulence (and where the loss terms are assumed to be equal to zero). The "poloidal" domain is half as wide as the "radial". All the simulations are performed with a 512x256 grid and are carried out until the turbulence reaches steady state and remains there for a statistically significant amount of time (i.e. the final time is thousands of correlation times). Although the output of the code is the full time dependent variation of all the scalar field evolved in Eqs.1-3, we focus here only on the decay length of the density, λ_n, temperature, λ_T and heat flux, λ_q. These are obtained in the following way. We started by averaging the density, $n(x,y,t)$, first over the poloidal direction and then over time (during the period of statistically steady turbulence). This allowed us to find a single time independent radial profile , $<n>$. We then constructed $\lambda_n = \rho_s <n> /(d<n>/dx)$, which is again a function of x. Note that the factor ρ_s is used to make the decay length dimensional (we express it in cm). Since the $<n>$ profile is not simply exponentially decaying, λ_n has a complex radial dependence. A possible way to characterise the width of the SOL with a scalar number, is to associate it with the local minimum of the decay length profile after the separatrix (a robust feature of our simulations). This is a good (but conservative) estimate as it represents the steepest gradient in a position where the SOL is dense and hot (and hence more likely to cause problems to the divertor). The same procedure applied to $T(x,y,t)$ gives λ_T.

It is now possible to identify the relation between the decay lengths and the dimensionless parameters using statistical techniques. The data can be treated with regression analysis by assuming the following form for a generic decay length: $\frac{\lambda_f}{R} = \alpha \left(\frac{\rho_s}{R}\right)^{\beta_1} D^{\beta_2} \chi^{\beta_3} \mu^{\beta_4} \Sigma_n^{\beta_5} \Sigma_T^{\beta_6}$. In the calculation, we removed the statistically irrelevant dimensionless parameter using the Student's t-test and repeated the regression without them (for this reason the viscosity dependence is not present in the following expressions). The resulting scaling laws for the decay length are:

$$\frac{\lambda_n}{R} = 1.04\exp(\pm 0.29)\left(\frac{\rho_s}{R}\right)^{1.09\pm 0.07} D^{0.71\pm 0.04}\Sigma_n^{-0.73\pm 0.04}\Sigma_T^{-0.19\pm 0.03} \quad (4)$$

$$\frac{\lambda_T}{R} = 1.91\exp(\pm 0.51)\left(\frac{\rho_s}{R}\right)^{1.07\pm 0.12} D^{0.31\pm 0.18}\chi^{0.14\pm 0.12}\Sigma_n^{-0.10\pm 0.07}\Sigma_T^{-0.52\pm 0.07}. \quad (5)$$

Both regressions give a good coefficient of determination, R^2 ($\mathsf{R}^2 = 0.98$ in both cases). Combining Eqs.1 and 2, we can find an expression for the evolution of the thermal power density (identified with the pressure), from which we find that $\nabla_\parallel q_\parallel = \frac{3}{2}(\Sigma_T + \Sigma_n)nT$, where $q_\parallel$ is the heat flux flowing in the parallel direction. We now take $\lambda_q \equiv \rho_s \int \overline{\nabla_\parallel q_\parallel} dx / [3/2(\Sigma_T + \Sigma_n)p_{sep}]$, where the overline represents poloidal average and p_{sep} is the normalized pressure at the separatrix. This integral definition is well suited to capture the power deposition and it is therefore preferred to the one we used for λ_T and λ_n. Applying regression analysis, we obtain:

$$\frac{\lambda_q}{R} = 2.08\exp(\pm 0.16)\left(\frac{\rho_s}{R}\right)^{1.18\pm 0.03} D^{0.28\pm 0.02}\Sigma_n^{-0.16\pm 0.03}\Sigma_T^{-0.48\pm 0.02}, \quad (6)$$

which gives again $\mathsf{R}^2 = 0.98$.

While Eqs.4-6 are the natural way to express how the decay lengths behave as a function of the parameters of the model, they still remain relatively obscure. In particular, it is useful to explicitly relate the λs to measurable quantities such as the magnetic field or the edge density. This can be straightforwardly done by replacing in Eqs.4-6 reasonable definitions for the dimensionless parameters in terms of engineering parameters. Unfortunately, this procedure relies on the specific choice of these definitions which are sometimes not completely rigorous due to lack of detailed models (for example no neoclassical diffusion model exists in open field lines). For arbitrary electron collisionality, ν_*, we have: $\frac{\rho_s}{R} \sim \frac{T_0^{1/2}}{BR}$, $D \sim \mu \sim \frac{q^2 n_0}{BT_0^{3/2}}$, $\Sigma_n \sim \frac{T_0^{1/2}}{LB}$, where T_0 and n_0 are evaluated at the inner radial boundary, q is the safety factor in the same position, L is the midplane to target connection length. The thermal diffusivity can change depending on the collisionality, so that: $\chi \sim \frac{q^2 n_0}{BT_0^{3/2}}$ if $\nu_* \ll 12$ or $\nu_* \gg 63$ and $\chi \sim \frac{q^2 n_0^2 L}{BT_0^{7/2}}$ if $12 < \nu_* < 63$. Similarly, $\Sigma_T \sim \frac{T_0^{1/2}}{BL}$ if $\nu_* \ll 4$ and $\Sigma_T \sim \frac{T_0^{5/2}}{n_0 BL^2}$ if $\nu_* \gg 4$. References [3, 4] discuss these approximations.

With these definitions, we find that (assuming $L \sim qR$):

$$\lambda_q \sim q^{1.18} n_0^{0.28} T_0^{-0.14} B^{-0.83} R^{0.44} \qquad \text{if } \nu_* \ll 4, \tag{7}$$

$$\lambda_q \sim q^{1.65} n_0^{0.75} T_0^{-1.08} B^{-0.84} R^{0.91} \qquad \text{if } \nu_* \ll 4, \tag{8}$$

while similar expressions can be straightforwardly derived for the density and temperature decay length from 4-5. Unfortunately, the edge plasma parameters that appear in Eqs.7-8 cannot be immediately translated into the engineering parameters, such as the power crossing the separatrix, P_{SOL} or the line averaged density, which can be directly controlled in experimental studies. While it is not possible to replace the edge density with its line averaged counterpart (ESEL does not describe the core physics), we can at least rewrite the previous scaling laws in terms of P_{SOL} (numerically measured). This gives:

$$\lambda_q \sim q^{1.52} n_0^{0.7} P_{SOL}^{-0.25} B^{-1.03} R^{0.91} \qquad \text{if } \nu_* \ll 4, \tag{9}$$

$$\lambda_q \sim q^{2.24} n_0^{2.28} P_{SOL}^{-1} B^{-1.78} R^{2.46} \qquad \text{if } \nu_* \gg 12. \tag{10}$$

The low collisionality expression, Eq.9, can be compared with recent experimental scaling laws obtained in similar regimes [5]. Despite the limitations of the model and of the procedure used, we find a reasonable agreement with the exponents of q and B as well as a weak dependence on the power crossing the separatrix. Interestingly, our results seem to miss the weak machine size dependence of the experimental scaling law.

This work was part-funded by the RCUK Energy Programme [grant number EP/I501045] and the European Communities under the contract of Association between EURATOM and CCFE. To obtain further information on the data and models underlying this paper please contact PublicationsManager@ccfe.ac.uk. The views and opinions expressed herein do not necessarily reflect those of the European Commission.

References

[1] O.E. Garcia, V. Naulin, A.H. Nielsen and J.J. Rasmussen, Phys. Rev. Lett. **92**, 165003 (2004).

[2] F. Militello, W. Fundamenski, V. Naulin, A.H. Nielsen, Plasma Phys. Control. Fusion **54**, 095011 (2012).

[3] F. Militello, V. Naulin, A.H. Nielsen, Plasma Phys. Control. Fusion in press (July 2013)

[4] W. Fundamenski, O.E. Garcia, V. Naulin *et al.*, Nucl. Fusion **47**, 417 (2007).

[5] A. Scarabosio, T. Eich, A. Herrmann, B.Sieglin, Paper P1-33 in Proceedings of the 20th International Conference on Plasma Surface Interactions, Aachen, May 2012.